STEM CELLS TRANSLATIONAL MEDICINE®

TISSUE ENGINEERING AND REGENERATIVE MEDICINE

Long-Distance Axonal Growth and Protracted Functional Maturation of Neurons Derived from Human Induced Pluripotent Stem Cells After Intracerebral Transplantation

JONATHAN C. NICLIS,[a*] CHRISTOPHER TURNER,[a*] JENNIFER DURNALL,[a] STUART MCDOUGAL,[a] JESSICA A. KAUHAUSEN,[a] BRYAN LEAW,[a] MIRELLA DOTTORI,[b] CLARE L. PARISH,[a] LACHLAN H. THOMPSON[a]

Key Words. Grafting • Regeneration • Connectivity • Forebrain • Electrophysiology

[a]Florey Institute for Neuroscience and Mental Health, Royal Parade, Parkville, Victoria, Australia; [b]Department of Electrical and Electronic Engineering, Centre for Neural Engineering, University of Melbourne, Royal Parade, Parkville, Victoria, Australia

Correspondence: Lachlan Thompson, PhD, Florey Institute for Neuroscience and Mental Health, Royal Parade, Parkville, Victoria, Australia. Telephone: 61 3 90356796; Fax: +61 3 90353107; e-mail: lachlant@unimelb.edu.au

*Contributed equally.

Received April 20, 2016; accepted for publication October 31, 2016; published Online First on February 15, 2017.

1066-5099/2016/$30.00/0

http://dx.doi.org/10.1002/sctm.16-0198

ABSTRACT

The capacity for induced pluripotent stem (iPS) cells to be differentiated into a wide range of neural cell types makes them an attractive donor source for autologous neural transplantation therapies aimed at brain repair. Translation to the in vivo setting has been difficult, however, with mixed results in a wide variety of preclinical models of brain injury and limited information on the basic in vivo properties of neural grafts generated from human iPS cells. Here we have generated a human iPS cell line constitutively expressing green fluorescent protein as a basis to identify and characterize grafts resulting from transplantation of neural progenitors into the adult rat brain. The results show that the grafts contain a mix of neural cell types, at various stages of differentiation, including neurons that establish extensive patterns of axonal growth and progressively develop functional properties over the course of 1 year after implantation. These findings form an important basis for the design and interpretation of preclinical studies using human stem cells for functional circuit re-construction in animal models of brain injury. STEM CELLS TRANSLATIONAL MEDICINE *2017;6:1547–1556*

SIGNIFICANCE STATEMENT

Neurons generated from human pluripotent stem cells can establish extensive patterns of connectivity in a host brain and survive for up to one year after transplantation. Functional maturation, assessed by patch-clamp recordings, occurs over months rather than weeks. These observations are significant for the design and interpretation of pre-clinical studies aimed at developing stem cell therapies for brain repair. They demonstrate in principle feasibility for anatomically reconstruction of long-distance circuitry but also highlight that therapeutic impact linked to functional integration will require sufficient post-transplantation observation times.

INTRODUCTION

One of the most anticipated clinical applications for induced pluripotent stem (iPS) cells is the functional replacement of damaged central nervous system (CNS) circuitry. The capacity of iPS cells to be differentiated into a wide variety of CNS cell types has stimulated significant research into their potential as a donor source for a range of neurological conditions characterized by neuronal cell loss. For example, there are now routine procedures for directed differentiation of human pluripotent cells into midbrain dopamine neurons relevant for cell-based therapy in Parkinson's disease (PD) [1], [2], [3] spinal motor neurons for motor neuron disease or acute spinal injury [4–6], medium spiny projection neurons for Huntington's disease [7–10], or cortical projection neurons [11, 12] that could replace damaged cortical circuitry after stroke or traumatic brain injury. A key challenge in this field is to translate this success at the in vitro level into reliable procedures for functional cell replacement in models of CNS damage.

Overall the therapeutic impact in human iPS-based neural transplantation studies has been highly variable and there has been lack of consensus on the underlying mechanisms (for review see [13]). For example, in models of PD there have been reports of modest recovery of simple motor function [14–16], while in models of stroke and spinal injury the results have been much more mixed (for reviews see [17–19]). A general limitation of work in this area has been a lack of detailed information on the functional and

anatomical characteristics of neural grafts generated from human iPS cells. This makes it difficult to link key features of the graft to the therapeutic impact.

In this study, we demonstrate the utility of a human iPS cell line constitutively expressing green fluorescent protein (GFP) as a tool for characterizing anatomical and functional features of neural grafts derived from iPS cells. Stable expression of GFP in all differentiated cell types up to 1 year after intracerebral transplantation into adult, athymic rats allowed us to chart the progressive development of electrophysiological properties of grafted neurons and to provide a detailed description of the anatomical patterns of long-distance axonal growth in the host brain. These results are consistent with recent studies using human embryonic stem (ES) cells [12, 20, 21] and highlight the protracted nature of functional maturation of neurons generated from human iPS cells as well as their remarkable capacity for long-distance axonal growth throughout the adult brain.

Materials and Methods

Cell Culture and Differentiation

iPS cells (iPS1, WiCell USA) were cultured as previously described [22] at 37°C, 5% CO_2 on mitomycin-C treated human foreskin fibroblasts in media consisting of DMEM/nutrient mixture F-12, supplemented with 0.1 mM β-mercaptoethanol, 1% nonessential amino acids, 2 mM glutamine, 25 U/ml penicillin, 25 μg/ml streptomycin and 20% knockout serum replacement, KSR (all from Invitrogen). The iPS-GFP cells were generated using the *piggyBac* transposon vector (Wellcome Trust Sanger Institute) modified to contain a GFP expression cassette, driven by the human elongation factor 1 alpha promoter. For neural induction, colonies were treated with human recombinant noggin (500 ng/ml, PeproTech) and basic Fibroblast Growth Factor, (bFGF, 4 ng/ml, R&D Systems) in neural basal media (NBM) [23]. After 11 days, colonies were mechanically harvested and cultured in suspension in NBM supplemented with 20 ng/ml bFGF and 20 ng/ml epidermal growth factor (EGF, R&D Systems) as neurospheres for a further 7 days, then dissociated into a single cell suspension using triple express medium (Invitrogen) and re-suspended at 1×10^5 cells per microliter in HBSS without Ca^{2+} or Mg^{2+}, supplemented with 0.05% DNase.

Animals and Transplantation

The use of animals in this study conformed to the Australian National Health and Medical Research Council's published Code of Practice for the Use of Animals in Research, and experiments were approved by the Florey Institute for Neuroscience and Mental Health Animal Ethics Committee. A total of 20 female athymic rats were used as transplant recipients, with 4 animals allocated to each of the three time-points for electrophysiological studies and the remaining 8 allocated for histological analysis at the study end point (50 weeks). Under deep anesthesia (2% isoflurane) each rat was placed in a stereotaxic frame (Kopf, Germany) and received an injection of 1×10^5 cells (differentiated for 18 days) in a volume of 1 μl using a glass cannula fitted to a 5 μl Hamilton syringe as previously described [24]. The cells were injected into the striatum (0.5 mm anterior and 2.5 mm lateral to Bregma, 4 mm below the dura) over 1 minute and the cannula left in place a further 2 minutes to minimize reflux. The animals were maintained on a normal 12 hours light/dark cycle in individually ventilated cages and low irritant bedding with ad libitum access to food and water for the remainder of the experiment.

Electrophysiology

Cortical Slice Preparation. Coronal forebrain slices were prepared from grafted rats 10, 26, and 50 weeks following implantation. Rats were deeply anesthetized with an overdose of isoflurane (100 mg/kg) and the brains were rapidly removed and cooled. Sections (200 μm) were collected at the level of the graft site using a vibrating microtome (VT1000S; Leica Microsystems Inc., Bannockburn, IL) and placed in artificial cerebrospinal fluid (aCSF) containing (mM): 125 NaCl, 3 KCl, 1.2 KH_2PO_4, 1.2 $MgSO_4$, 25 $NaHCO_3$, 10 dextrose and 2 $CaCl_2$ (300 mOsmol). At 30°C, bubbled with 95% O_2 − 5% CO_2. For recordings slices were secured with a nylon mesh and perfused with aCSF at 32°C–34°C, bubbled with 95% O_2 and 5% CO_2.

Whole Cell Electrophysiology. Recording pipettes (3.2–4.5 MΩ) were guided to iPS cells identified by GFP in the striatum or overlying cortex. Neurons were visualized using Dodt gradient contrast (x40 water immersion lens) and filter set 38 on an Axio Examiner fixed stage microscope (Zeiss, Thornwood, NJ) with digital camera (Rolera EM-C^2, Q imaging, Surrey, BC). Pipettes were filled with a low Cl^- intracellular solution containing (mM): 6 NaCl, 4 NaOH, 130 K-gluconate, 11 EGTA, 1 $CaCl_2$, 1 $MgCl_2$, 10 HEPES, 2 Na_2ATP, and 0.2 Na_2GTP Na_2GTP and 0.5% biocytin (pH 7.3 and 296 mOsm). As a consequence, $E_{Cl} = -69$mV, inhibitory postsynaptic currents (IPSCs) had small amplitudes at $V_H = -60$mV, though more prominent outward current amplitudes were achieved by shifting to $V_H = -40$mV in some cases. All recordings were made in open, whole cell patch configuration under voltage clamp using a Multiclamp 700B (Molecular Devices, Sunnyvale, CA). Signals were sampled at 20 kHz and filtered at 10 kHz using p-Clamp software (version 10.3, Molecular Devices, Sunnyvale, CA). After recordings, slices were fixed in 4% PFA and incubated for 2 hours with streptavidin-555 (ThermoFisher) diluted 1:500 in PBS. *Voltage clamp measurements*. Cells were held at −60 mV and inward spontaneous excitatory postsynaptic currents (EPSCs) were recorded for 3 minutes. Cells were held at −40 mV and outward spontaneous IPSCs were recorded for 3 minutes.

Membrane Potential Measurements. Action potentials (APs) were stimulated in current-clamp mode. Resting membrane potential was recorded over 1 minute. Membrane potential adjusted to −60 mV (current subtraction -6 ± 2 pA for all cells) and cells depolarized with a series of 400–1000 ms current pulses in 20 pA increments up to 260 pA.

Data Analysis and Statistics. For input-ouput curves, APs were counted over the step period and groups compared by two-way ANOVA with Student-Newman-Keuls post hoc. Proportions of iPS cells that exhibited AP failures in response to a 260 pA step were compared by *z* test. Spontaneous EPSC frequency and amplitudes were compared by one-way ANOVA with Dunn's post hoc. Proportions of iPS cells that exhibited spontaneous excitatory postsynaptic currents (sEPSCs) were compared by *z* test.

Immunohistochemistry

Fifty weeks after transplantation, animals received a lethal dose of pentobarbitone and were trans-cardially perfused with 50 ml saline (0.9% wt/vol) followed by 200–250 ml paraformaldehyde

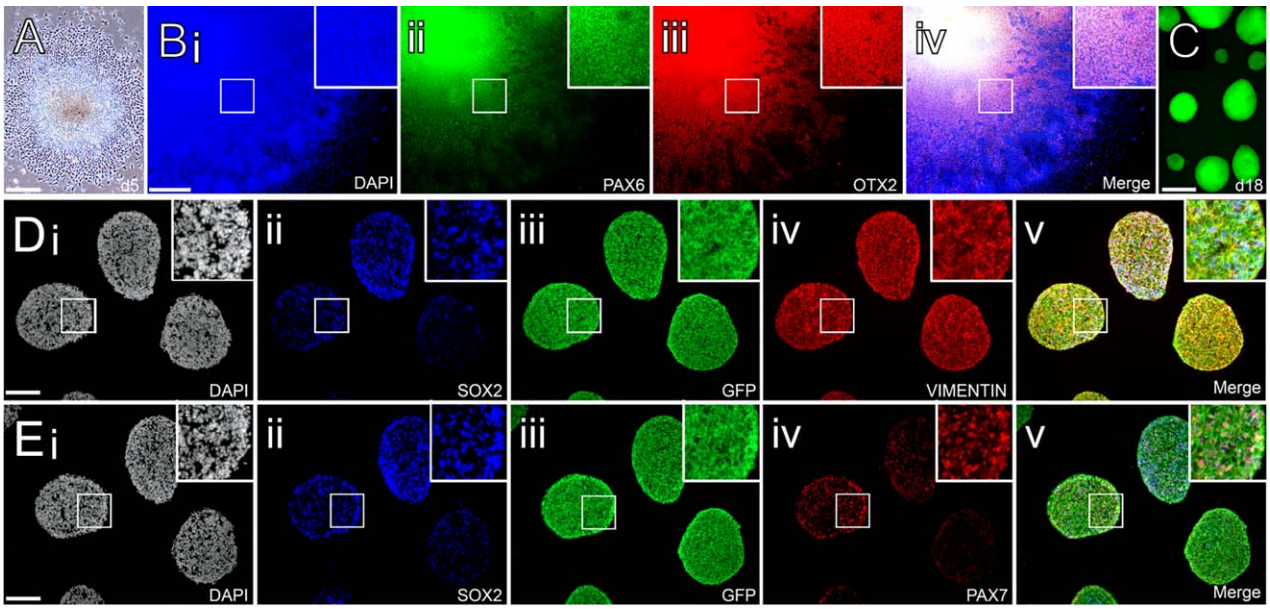

Figure 1. Neural induction of human induced pluripotent stem cells constitutively expressing GFP. **(A)**: Phase contrast image showing colony formation with typical neuroepithelial morphology after 5 days of neural induction. **(Bi–Biv)**: Colonies at 11 days express regional markers PAX6 and OTX2 consistent with a dorsal forebrain progenitor phenotype. **(C)**: At the time of transplantation (day 18), native GFP can be readily visualized in live neurospheres generated from the center of neuroepithelial colonies. **(Di–Dv)**: Cryosectioned spheres show uniform cytoplasmic expression of GFP and widespread expression of neural progenitor markers including Sox2 and Vimentin. **(Ei–Ev)**: Many of the Sox2+ neural progenitors also expressed the dorsal marker Pax7 at the time of transplantation. Scale bars: A, C–1 mm; B, 500 μm; D, E 400 μm. Abbreviation: GFP, green fluorescent protein.

(PFA; 4% wt/vol in 0.1 M phostphate buffered saline (PBS)). The brains were removed, postfixed a further 2 hours in PFA and cryoprotected in sucrose (25% wt/vol in 0.1 M PBS). Brains were sectioned in the coronal or horizontal plane in 12 series at a thickness of 30 μm on a freezing microtome (Leica, Germany). Immunohistochemistry on free-floating sections was as previously described [25]. Primary antibodies and dilution factors were as follows: goat anti-doublecortin (DCX, 1:400; SCBT), rabbit anti-GABA (1:2,500; Sigma), rabbit anti-GFAP (1:200; DAKO), chicken anti-GFP (1:1,000; AbCam), rabbit anti-GFP (1:20,000; AbCam), rabbit anti-Ki67 (1:1,000; ThermoFischer), mouse anti-NeuN (1:1,000; Millipore), rabbit anti-Otx2 (1:500; Millipore), mouse anti-Pax7 (1:80; DSHB), mouse anti-Pax6 (1:100; DSHB), goat ant-Sox2 (1:100; R&D Systems), rabbit anti-TBR1 (1:100; Millipore), mouse anti-VGLUT2 (1:500; Millipore), rabbit anti-Vimentin (1:500; Abcam) . For DAB-based detection of GFP, a biotinylated goat anti-rabbit secondary anti- body (Vector Laboratories) was subsequently conjugated with streptavidin-HRP using the Vectastain ABC Elite kit (Vector Laboratories). For immunofluorescence detection, species-specific secondary antibodies generated in donkey and conjugated with the Dylight range of fluorophores with various peak emission wavelengths including 488, 549, and 633 were used at a dilution of 1:500 (Jackson ImmunoResearch).

Imaging and Histological Quantification

Fluorescent images were captured using a Zeiss Meta laser scanning confocal upright microscope. To provide macroscopic illustrations of GFP immunoreactivity, montages of single darkfield images captured using a ×20 objective were constructed using a Leica DM6000 B upright light microscope equipped with a motorized stage. The sections and GFP+ fiber patterns were reconstructed by tracing over the montaged images using Canvas software (ACD systems). Morphological profiles of biocytin filled cells were generated by accurately tracing over collapsed *z*-stacks of the streptavidin-555 labeled dendrites using Adobe photoshop software.

Graft volumes were estimated through extrapolation of the area of GFP measured in every 12th section according to Cavalieri's principle [26]. The cellular densities of the grafts were estimated through counting of DAPI-labeled nuclei in three separate ×40 (225μm^2) fields of view for each graft in five animals. The proportion of NeuN and TBr1 expressing neurons in three of the grafts was estimated by inspection of every DAPI cell in three separate ×20 (425μm^2) fields of view in each of three grafts.

Results

Rapid Neural Induction and Acquisition of Regional Identity of Human iPS Cells Stably Expressing GFP

Upon neural induction, human iPS cells formed colonies with characteristic neuroepithelial morphology by d5 (Fig. 1A) that were then treated with FGF2 to promote the expansion of neural progenitors. This resulted in colonies enriched for early telencephalic transcription factors, including the forebrain/midbrain regional marker OTX2 and dorsal forebrain marker PAX6 (Fig. 1B). These colonies were manually dissected to generate neurospheres that robustly express GFP at the time of transplantation (Fig. 1C). Immuno-labeling of cryosectioned neurospheres fixed at the time of transplantation showed cytoplasmic distribution of GFP ubiquitously throughout the spheres as well as proteins indicative of an early neural progenitor phenotype, including SOX2 and Vimentin (Fig. 1D) and Pax7 (Fig. 1E) consistent with dorsal regional identity.

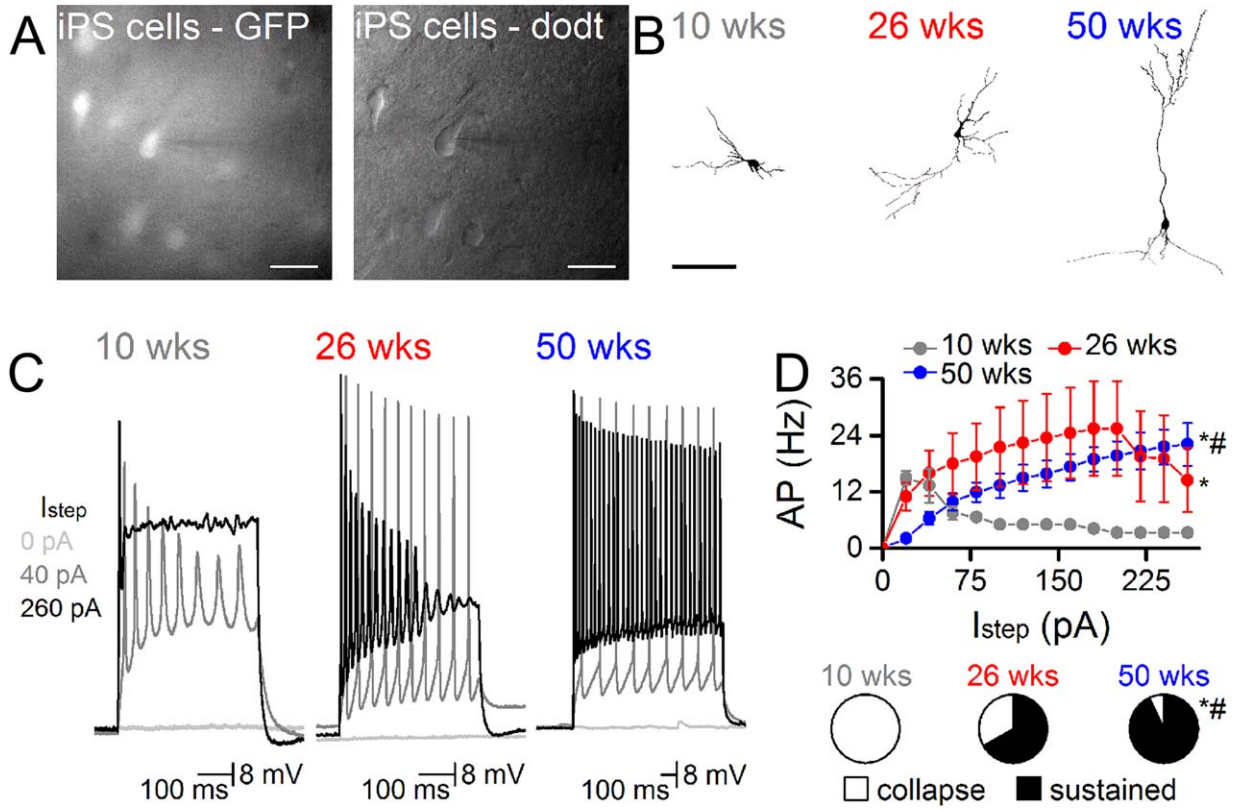

Figure 2. Neurons derived from human induced pluripotent stem (iPS) cells progressively develop functional properties over the course of 1 year after implantation into the adult rat brain. **(A)**: iPS derived cells were identified by GFP expression and targeted for whole cell recordings (pipette from right, scale = 20 μm). Pipettes contained biocytin to fill neurons. **(B)**: Representative examples of biocytin filled neurons at 10, 26, and 50 weeks show the progressive development of more complex morphological features, including some with pyramidal profiles by 50 weeks (scale 100 μm). **(C)**: APs firing became increasingly frequent and reliable the longer iPS cells remained in vivo. Representative traces from neurons at each time point show the depolarization response to 0, 40, and 260 pA steps. **(D)**: Input/output curves show the greater capacity to sustain increasing currents at the later in vivo time-points ($n = 6$ at 10 weeks, $n = 5$ at 26 weeks, $n = 14$ at 50 weeks). Pie-charts show the proportion of cells with sustainable APs at 260 pA (*, $p < .05$ vs. 10 week, #, $p < .05$ vs. 26 week, two way ANOVA). Abbreviations: AP, Action potentials; GFP, green fluorescent protein; pA, amplitude.

Progressive Electrophysiological Maturation of iPS Cell-Derived Neurons In Vivo

For electrophysiological assessment of grafted neurons, coronal slices were prepared 10, 26, and 50 weeks after transplantation. Native GFP fluorescence allowed for rapid identification of grafted cells, which were patched for whole cell recordings under dodt contrast in all slices (Fig. 2A). Representative reconstructed images of biocytin filled cells at 10, 26, and 50 weeks after transplantation showed a progressive maturation of neuronal morphology, most notably though the more prominent dendritic branching and spine density at 50 weeks (Fig. 2B). All recorded cells exhibited neuron-like resting membrane potentials (10 weeks, -56 ± 2 mV, $n = 6$; 26 weeks, -69 ± 3 mV, $n = 5$; 50 weeks, -67 ± 2 mV, $n = 14$). At the early 10-week postgraft time-point half of the cells failed to generate an APs response to current injections (Fig. 2C, 2D). We did, however, observe 3 out of 6 cells that were able to generate low amplitude APs that collapsed at higher ($\geq$60 pA) current injections (Fig. 2D). At 26 weeks, recordings in 5 cells produced APs that were notably more robust in terms of amplitude and fired at higher frequencies with current injections although an overall heterogeneous input/output response was noted, with 3 cells sustaining regular AP firing up to 260 pA while 2 exhibited a collapsing pattern similar to the cells recorded at 10 weeks (Fig. 2C, 2D). At 50 weeks, observations in 14 GFP+ cells showed that the main distinction relative to the earlier time-points was the consistency of the input/output response with 13 of 14 cells able to sustain regular high amplitude AP firing with increasing frequency in response to current steps up to 260 pA (Fig. 2C, 2D). This suggests by 50 weeks, post implantation, the majority of iPS cells expressed a sufficient voltage activated ion channel density to support this high intensity output.

To assess if iPS cell derived neurons receive functional afferent input, voltage clamp recordings were also performed in the same neurons at each post-transplantation time-point. At 10 weeks, there was no evidence of sEPSCs in any of the 6 cells (Fig. 3A, 3B). At 26 weeks, 2 of 5 cells exhibited sEPSCs at low frequency (0.03 ± 0.02 Hz) but with high amplitude (48 ± 6 pA). By 50 weeks post-transplantation, sEPSCs were observed in all 14 GFP+ cells and these occurred at greater frequency (1.4 ± 0.3 Hz) compared to earlier time points but were not different in amplitude to sEPSCs at 26 weeks (Fig. 3B). In one of these 50 week cells, we also observed inhibitory postsynaptic currents (0.7 Hz, 20 pA–not shown).

Long-Term Survival and Extensive Axonal Growth from Neural Grafts Derived from Human iPS Cells

Histological analysis 50 weeks after transplantation showed that expression of GFP was maintained uniformly throughout the

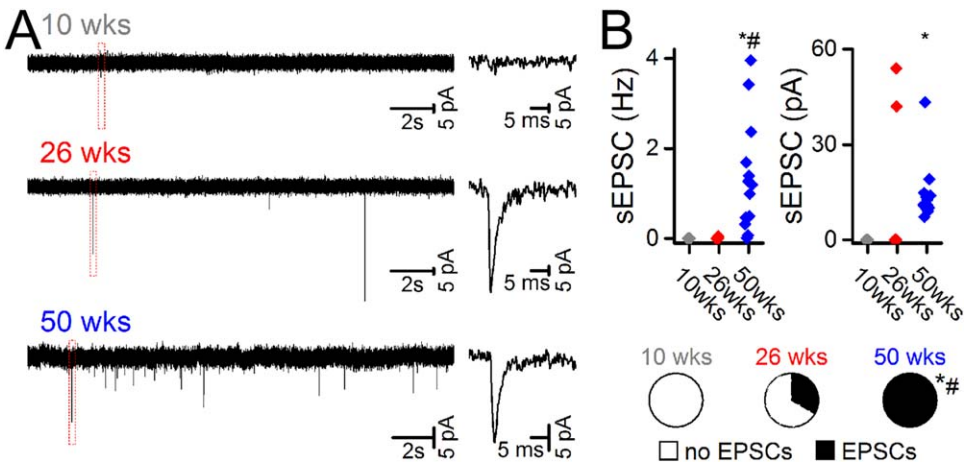

Figure 3. Neurons derived from human induced pluripotent stem cells exhibit properties of synaptic integration in vivo. **(A)**: Representative traces from neurons in voltage clamp at each time point demonstrating sEPSCs at 26 and 50 weeks. **(B)**: Accompanying graphs show the frequency (Hz) and amplitude (pA) of sEPSCs in recorded cells at each time-point, as well as the proportion of cells exhibiting sEPSCs (*, $p < .05$ vs. 10 week, #, $p < .05$ vs. 26 week, one way ANOVA or *z* test). Abbreviations: EPSCs, excitatory postsynaptic currents; sEPSCs, spontaneous excitatory postsynaptic currents.

grafted iPS cells. Grafts were present as discrete deposits in the dorsal head of the striatum as well as the overlying corpus callosum and frontal cortex. In some animals, reflux of the cells along the injection tract meant that the graft deposit was contained entirely within the cortex, rather than the striatal target site (e.g., Fig. 4A). The graft volumes were highly variable (8.86 ± 4.84 mm^3) and thus so were the total number or DAPI+ cells ($2.19 \pm 1.24 \times 10^6$), representing on average an approximate 20-fold increase from the original donor preparation of 1×10^5 cells per animal. Even at the 50-week time-point there was a persistence of immature neural cell types, including small clusters of doublecortin+/GFP+ cells with neuroblast morphology that had migrated a short distance into the adjacent host cortex (Fig. 4B) and dividing Ki67+/Sox2+ progenitors within the graft core (Fig. 4C). There were also examples of individual GFP+ cells with more mature morphological profiles consistent with terminally differentiated neurons and glia that had migrated from the graft into the adjacent host parenchyma (Fig. 4D).

Labeling for glial fibrillary acidic protein (GFAP) revealed some examples of GFAP+/GFP+ cells (Fig. 4E), however the filamentous nature of GFAP labeling made it difficult to estimate the proportion of these cells within the grafts. Double-labeling with NeuN showed a substantial number of GFP+ cells with mature neuronal identity (Fig. 4F). These cells were distributed in a non-uniform manner throughout the grafts, with dense clusters of NeuN+ cells interspersed with areas sparsely populated with NeuN+ cells. Counting of NeuN+ cells by sampling from multiple fields of view within each graft revealed that $17.45\% \pm 2.2\%$ of grafted (DAPI+/GFP+) cells were NeuN+ neurons. Labeling with other phenotypic markers indicated that some of these neurons had a dorsal forebrain identity, with $17.45\% \pm 2.2\%$ of GFP+/NeuN+ cells coexpressing Tbr1 (Fig. 4F). We also observed as well as heterogeneously distributed pockets of cells densely labeled for Otx2 and/or Pax7 (Fig. 4G), however these were largely not NeuN+, possibly representing the persistence of dorsal forebrain and midbrain progenitor cells in the mature grafts.

In terms of neurochemical phenotype of the grafted neurons, we did not observe any evidence of neurons with dopaminergic (TH), cholinergic (ChAT) or serotonergic (5HT) identity (not shown). We did, however, observe numerous GABA+/GFP+ neurons and dendrites throughout the grafts (Fig. 4H) as well as a dense pattern of punctate labeling for the vesicular glutamate transporter VGLUT2 (Fig. 4I, 4J). Although within the graft core it was not possible to unambiguously associate the VGLUT2+ with grafted cells (as opposed to innervating host fibers), close inspection of individual GFP+ fibers coursing through white matter tracts showed at least some of the grafted neurons colabeled for VGLUT2 (Fig. 4J).

One of the most striking aspects of the histological analysis was the capacity for grafted neurons to establish extensive patterns of long-distance axonal growth throughout the host brain. A conspicuous feature was the propensity for axonal growth along host white matter tracts of the external and internal capsules. Large numbers of GFP+ axons extended medio-laterally, across both hemispheres, via the corpus callosum and anterior commissure (Fig. 5A, 5J) and also throughout the rostro-caudal axis via the external capsule and myelinated fiber bundles of the internal capsule (Fig. 5A–5C). In the rostral direction, fibers extended through forceps minor and could be found as far as the olfactory bulb (Fig. 5D). Growth caudal to the graft was extensive, travelling long distances along the internal capsule, ventrally through the entopeduncular nucleus (Fig. 5A, 5F) and cerebral peduncles (Fig. 5A, 5G) and into the brainstem (Fig. 5A). Dorsally, GFP+ fibers coursed along the superior cerebellar peduncle and into the arbor vitae of the cerebellum (Fig. 5A, 5E).

Innervation of specific host nuclei was most prominent proximal to white matter corridors, particularly in cortical areas including those adjacent to the ventral extremities of the external capsule (Fig. 5A, 5H) and overlying the corpus callosum and forceps minor (Fig. 5A, 5I). Fibers also exited the corpus callosum ventrally into the septum (Fig. 5A 5J). Few fibers were observed to innervate thalamic nuclei, although there was a prominent passaging of fibers medial from the entopeduncular nucleus toward the hypothalamus (Fig. 5M). Immediately adjacent to the graft in the striatum, high magnification images showed dense fiber networks with a punctate pattern consistent with terminal ramification (Fig. 5A, 5K, 5L).

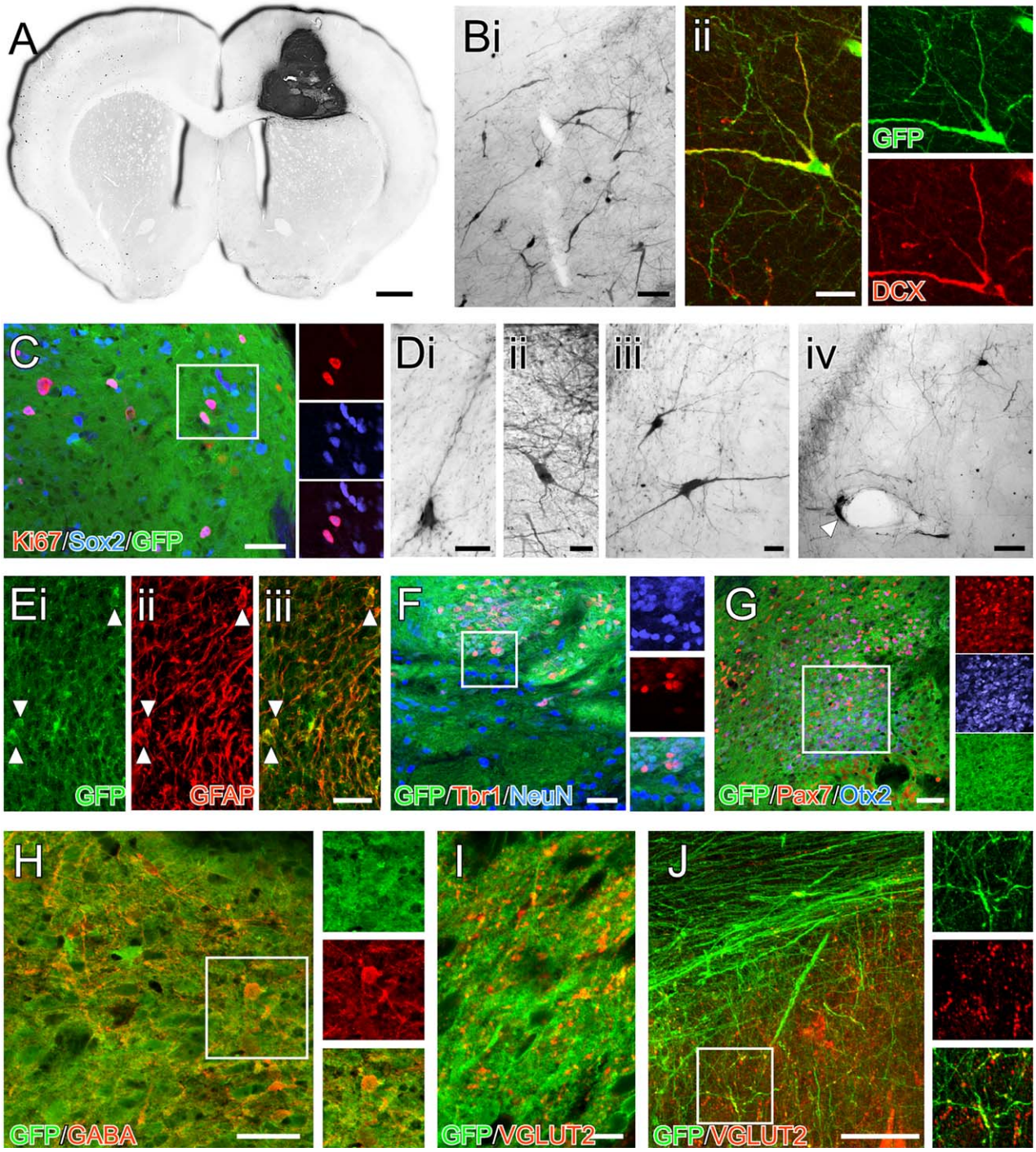

Figure 4. Composition of neural grafts generated from human induced pluripotent stem cells 50 weeks after transplantation. **(A)**: Immunohistochemistry for GFP in a coronal section shows an example of a graft contained within the host cortex and corpus callosum. **(B)**: Cells with the morphology of migrating neuroblasts could be found in the adjacent host parenchyma **(Bi)** and many of these cells colabeled with doublecortin **(Bii)**. **(C)**: Other immature neural cell types persisted in the grafts at 50 weeks including Sox2+ progenitors, some of which were actively dividing based on Ki67 expression (boxed area shown as separate color channels). **(D)**: Many of the cells also had more differentiated morphology, some with neuronal profiles **(Di–Diii)** while others with glial morphology were often found in close proximity to host blood vessels (**Div**; arrow). **(E)**: Labeling for GFAP showed a strong filamentous pattern of GFAP+ throughout the grafts including a number GFAP+/GFP+ cell bodies. **(F)**: NeuN and Tbr1-expressing GFP+ cells could be found throughout the grafts, although the distribution was nonuniform—this image shows one of the regions with a high frequency of these cells (boxed area shown as separate color channels). **(G)**: Other transcription factors associated with dorsal forebrain identity, including Otx2 and Pax7 were also found in restricted areas as discrete clusters in the grafts (boxed area shown as separate color channels). **(H)**: In terms of neurochemical identity, GABA+/GFP+ cells could be found throughout the grafts and VGLUT2 immunoreactivity **(I)** was also prevalent with a punctate pattern of labeling throughout all grafts (note the cell nuclei as dark areas lacking cytoplasmic GFP for scale reference). **(J)**: Analysis of individual GFP+ fibers (here in the corpus callosum) showed colocalization of VGLUT2 (boxed area enlarged as separate color channels). Scale bars: A–1 mm; Bi, Div, E, F, G, H, J–50 μm; Bii, Di–Diii, I–20 μm. Abbreviation: GFP, green fluorescent protein.

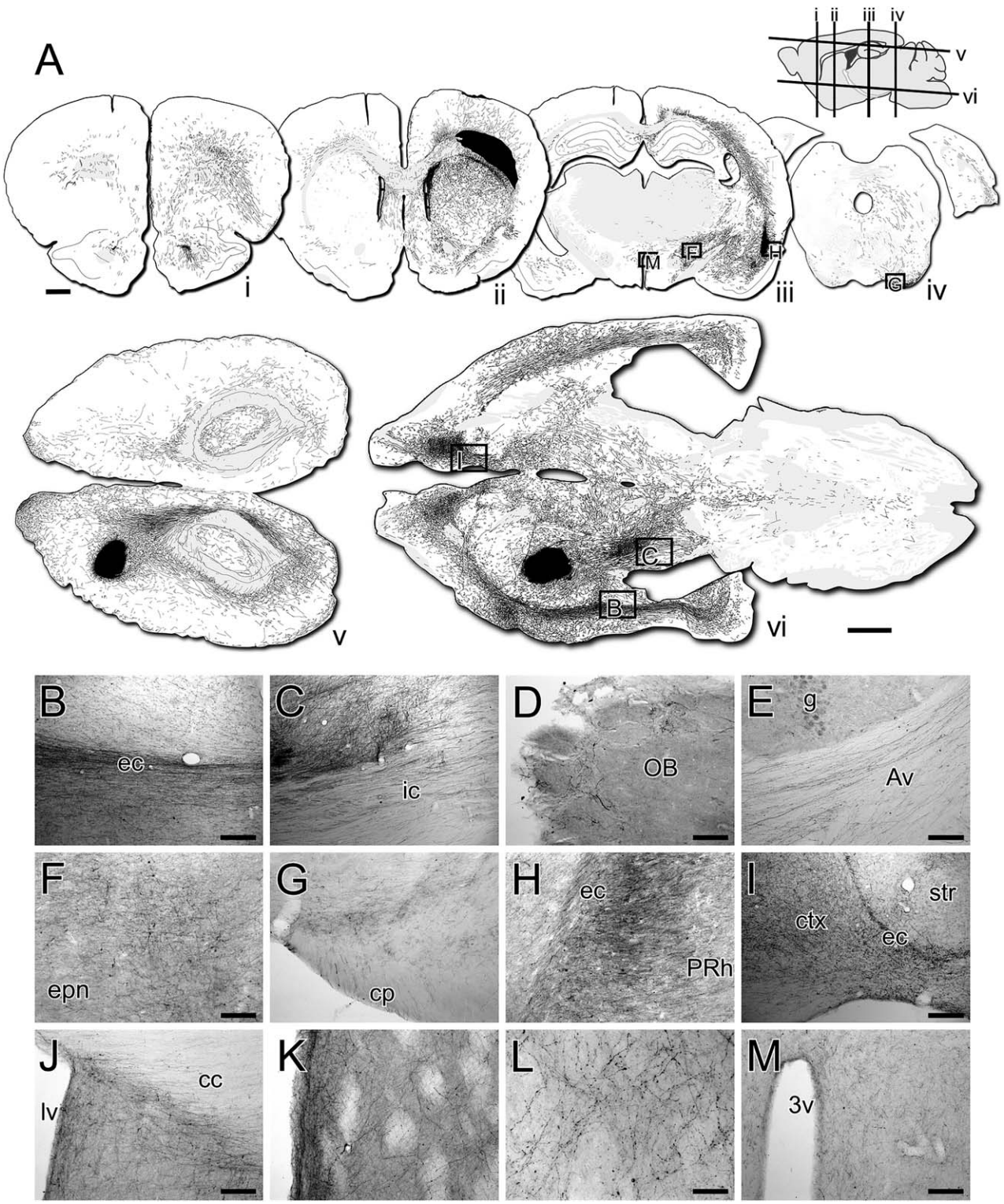

Figure 5. Long-distance fiber growth of grafted neurons throughout the host brain. **(A)**: Reconstructions of darkfield photo-montages of coronal (**A-i–A-iv**, top row) and horizontal (**A-v, A-vi**, bottom) sections labeled for GFP 50 weeks after transplantation. The GFP+ fibers were carefully traced over by hand. The graft appears as a black deposit in the corpus callosum (section ii) or the striatum and overlying cortex (sections A-v, A-vi). Approximate location of the section planes are shown in the sagittal section (top right). Brightfield images of DAB-labeled immunohistochemistry for GFP from the same sections (boxed) used for the reconstructions show GFP+ fibers: coursing through host white matter tracts including the external capsule **(B)** and internal capsule **(C)**; extending into the olfactory bulb **(D)**; in the arbor vitae of the cerebellum **(E)**; extending caudally through the entopeduncular nucleus **(F)** and cerebral peduncles **(G)**; innervating cortical areas adjacent to the external capsule, including the perirhinal cortex **(H)** and frontal cortical areas rostral to forceps minor **(I)**; coursing between hemispheres though the corpus callosum and ventrally into the septum around the midline **(J)**; innervating the striatum **(K)** with a punctate pattern of terminal ramification **(L)**; and running medially from the internal capsule toward the hypothalamus **(M)**. Abbreviations: 3v, third ventricle; Av, arbor vitae; cc, corpus callosum; ctx, cortex; ec, external capsule; ic, internal capsule; lv, lateral ventricle; OB, olfactory bulb; PRh, perirhinal cortex. Scale bars: A–1mm (both); B, C, E, I–200 μm; D, F, G, H, J, K, M–100 μm; L–50 μm.

Discussion

These results demonstrate that neurons generated from human iPS cells can survive up to 1 year after transplantation into the fully developed brain, where they develop functional electrophysiological properties and can form widespread patterns of long-distance axonal growth. The total number of cells in the grafts represented an increase ranging between ~4- to 30-fold compared to the original 1 x 10^5 cells grafted, demonstrating significant proliferation and net growth subsequent to transplantation. Indeed, even at 50-weeks there was a persistence of actively dividing Ki67+/Sox2+ neural progenitors.

The cytoplasmic distribution of GFP showed distinct neuronal morphologies, some with pyramidal appearance, while there were also clusters of bipolar neuroblasts around the periphery of the graft, suggesting on-going neurogenesis even up to 1 year after grafting. This extends on previous studies using human ES cells, showing the persistence of neural progenitors 3 months after grafting [20, 27]. Clusters of Otx2 and Pax7 expressing cells suggest the persistence of progenitors with dorsal mid/forebrain identity. The grafts also displayed properties that suggested at least some of the neurons may have acquired a cortical projection phenotype, including dendritic VGLUT2+ expression and large numbers of Tbr1 expressing cells. This would be consistent with previous reports showing a "default" differentiation of human pluripotent stem cells toward dorsal forebrain cell types under minimalist neural induction conditions [20, 28, 29].

A significant feature of the in vivo properties of the grafts was the remarkable growth of GFP+ fibers over long distances in the adult brain. This follows findings from similar studies using human ES cells, showing grafts of dorsal forebrain progenitors implanted into the frontal cortex of Non-Obese Diabetic/severe combined immune deficiency (NOD/SCID) mice establish extensive patterns of axonal growth, including innervation of midbrain and hindbrain targets [12, 27] and grafts of ventral midbrain progenitors implanted into the midbrain of athymic rats establish long-distance patterns of axonal connectivity with striatal and cortical forebrain targets [21]—for review see [13]. Here we report that neurons generated from iPS cells share this capacity for long-distance axonal growth in the fully developed brain. One of the most conspicuous features of the GFP+ growth pattern was the tendency for axonal extension along host white matter corridors. This included projections into the contralateral cortex, via the corpus callosum, as well as extensive growth caudally along the internal capsule and into the brainstem. These patterns are similar to those reported following grafting of human ES cell-derived dorsal forebrain progenitors into the neonatal [20] or adult [12, 27] rodent forebrain.

This may simply reflect a permissive growth trajectory given the close proximity of the grafts to major white matter structures including the corpus callosum. It is difficult to confidently distinguish between such passive growth properties and cell-intrinsic patterns of target-directed growth. Retrograde tracing studies by Espuny-Camacho et al. [12] support the idea that at least some component may represent cell-intrinsic growth preference by showing that grafted neurons corresponding to different cortical layers maintained distinct growth trajectories appropriate to their normal developmental targets. As we have discussed previously [13], the overall pattern of growth will likely reflect both target-directed outgrowth but also growth of unspecified progenitors that may take their cues from the host environment. Furthermore, any component of directed growth likely reflects the presence of various neuronal subtypes. Here we found that, using a procedure for rapid neural induction and relying on "default" acquisition of regional identity, the resulting grafts were of mixed composition, with only a minor proportion of cells that could be defined on the basis of molecular markers of phenotype, including Tbr1+/NeuN+ neurons that may represent dorsal forebrain (cortical projection) neurons. Thus, the innervation of known cortical projection targets including the contralateral cortex, striatum, and brainstem may reflect the presence of cortical projection neurons. Lack of innervation of other major cortical projection targets, such as thalamus, may suggest the absence of the corresponding cortical subtypes under these differentiation conditions. Further studies, including retrograde tracing approaches, will be of great benefit as a means to further characterize the origins of innervation of specific host nuclei according to neuronal phenotype.

At a functional level, transplanted neurons were able to acquire mature electrophysiological properties including sustained firing of APs in response to increasing current steps as well as evidence of afferent synaptic input. Both the intrinsic firing properties and also the capacity to support afferent input, based on frequency of sEPSCs under voltage clamp, showed a markedly protracted time-course of development over 1 year. The maturation state of the cells was clearly distinguishable at the 10, 26, and 50-week time-points. This is consistent with transplantation studies using human ES cells, where ex vivo recordings show an immature phenotype at 6–12 weeks but more complex firing patterns from 18 weeks onward [12, 20, 30]. In the study by Espuny-Camacho et al. [12], ES derived cortical neurons continued to mature up to 9 months in terms of both their electrophysiological properties and also at the anatomical level based on increased innervation of the host brain and development of dendritic complexity. Similarly, Steinbeck et al. [27] reported a progressive maturation of human ES cell grafts between 12 and 48 weeks in terms of the relative contribution of mature (NeuN) and immature (Ki67+, Nestin+) cell types. More recently, Avaliani et al. [31] showed that neurons generated from human iPS cells have immature intrinsic electrophysiological profiles and do not accommodate functional afferent input from the host after 6 weeks of coculture on mouse organotypic hippocampal slices. However, when grafted into athymic rats and examined at 24 weeks, path clamped human neurons display more mature membrane resistance and firing properties and receive functional input from the host. Taken together with the present results, it suggests that the functional maturation was not determined by differences in the mouse organotypic and rat transplantation models but rather is a general feature of neurons generated from human pluripotent stem cells.

While the capacity of these cells to acquire intrinsic functional properties in vivo is encouraging for cell replacement strategies for brain repair, a remaining challenge is the convincing demonstration that their projection pathways can functionally innervate specific host nuclei. At the ultrastructural levels at least, the human ES grafting studies by Steinbeck et al. [27] made use of human-specific synaptophysin antibodies to provide convincing demonstration of synaptic coupling of grafted human neurons with rodent host neurons. The development of technology to selectively stimulate or inhibit grafted neurons, for example, via optogenetics or manipulation through DREADDs, should further aid in the assessment of functional connectivity. These approaches have already been used to study the integration of human ES cell derived neurons in rodent models, including inhibitory

interneurons grafted into the hippocampus [32] and midbrain dopamine neurons grafted into the striatum (Steinbeck et al. 2015).

Conclusion

In summary, these results show that neural grafts generated from human iPS cells survive up to 1 year - a clinically relevant timeframe for cell replacement based therapies in patients - develop mature functional properties and establish extensive patterns of long-distance axonal growth throughout the host brain. These observations form an important basis for further studies aimed at understanding the relationship between the in vivo properties of grafted neurons and therapeutic outcome following transplantation in models of CNS injury. In particular, detailed information on anatomical integration properties through the use of reporter lines, and using human specific antibodies to polysialylated nuclear cell adhesion molecule. as recently demonstrated by[21], will allow for a more conclusive insight into the importance of innervation of specific host nuclei than has previously been shown in transplantation studies using human pluripotent cells[13]. Overall, the in vivo properties of neurons generated from human iPS cells appear similar to those already reported in similar studies using ES cells[12, 20, 27], including a protracted maturation period over months. This has important implications for the design and interpretation of pre-clinical studies aimed at cell replacement in animal models of brain injury. It suggests that rapid therapeutic impact after transplantation, as has been reported in models of stroke and trauma [33–40], is likely due to mechanisms not related to functional cell replacement such as neuroprotection or stimulation of host plasticity. Demonstration of therapeutic impact that may be attributable to *bone fide* circuit reconstruction should be based on sufficiently long observation periods and, ideally, detailed descriptions of the capacity of the grafts to reconstruct specific neuronal pathways relevant to the status of injury.

Acknowledgments

We thank Mong Tien and Haoyao Guo for expert technical assistance. C.P. is a Viertel Senior Research Fellow. This work was supported NHMRC project Grant 1042584. The Florey Institute of Neuroscience and Mental Health acknowledges the strong support from the Victorian Government and in particular the funding from the Operational Infrastructure Support Grant.

Author Contributions

J.N., C.T., J.D., and S.M.: collection and/or assembly of data, data analysis and interpretation, manuscript writing, final approval of manuscript; J.K.: collection and/or assembly of data. B.L.: collection and/or assembly of data; M.D.: conception and design, provision of study materials, final approval of manuscript; C.P.: conception and design, collection and/or assembly of data, data analysis and interpretation, manuscript writing, final approval of manuscript; L.T.: conception and design, financial support, collection and/or assembly of data, data analysis and interpretation, manuscript writing, final approval of manuscript.

Disclosure of Potential Conflicts of Interest

The authors indicated no potential conflicts of interest.

References

1 Kriks S, Shim JW, Piao J et al. Dopamine neurons derived from human ES cells efficiently engraft in animal models of Parkinson's disease. Nature 2011;480:547–551.

2 Kirkeby A, Grealish S, Wolf DA, et al. Generation of regionally specified neural progenitors and functional neurons from human embryonic stem cells under defined conditions. Cell Rep 2012;1:703–714.

3 Niclis JC, Gantner CW, Alsanie WF, McDougall SJ, Bye CR, Elefanty AG, Stanley EG, Haynes JM, Pouton CW, Thompson LH, Parish CL. Efficiently Specified Ventral Midbrain Dopamine Neurons From Human Pluripotent Stem Cells Under Xeno-Free Conditions Restore Motor Deficits in Parkinsonian Rodents. Stem Cells Transl Med 2016. pii: sctm.2016-0073.

4 Wichterle H, Lieberam I, Porter JA et al. Directed differentiation of embryonic stem cells into motor neurons. Cell 2002;110:385–397.

5 Lee H, Shamy GA, Elkabetz Y et al. Directed differentiation and transplantation of human embryonic stem cell-derived motoneurons. Stem Cells 2007;25:1931–1939.

6 Peljto M, Dasen JS, Mazzoni EO et al. Functional diversity of ESC-derived motor neuron subtypes revealed through intraspinal transplantation. Cell Stem Cell 2010;7:355–366.

7 Ma L, Hu B, Liu Y et al. Human embryonic stem cell-derived GABA neurons correct locomotion deficits in quinolinic acid-lesioned mice. Cell Stem Cell 2012;10:455–464.

8 Delli Carri A, Onorati M, Lelos MJ et al. Developmentally coordinated extrinsic signals drive human pluripotent stem cell differentiation toward authentic DARPP-32+ medium-sized spiny neurons. Development 2013;140:301–312.

9 Arber C, Precious SV, Cambray S et al. Activin A directs striatal projection neuron differentiation of human pluripotent stem cells. Development 2015;42:1375–1386.

10 Yuan F, Fang KH, Cao SY et al.. Efficient generation of region-specific forebrain neurons from human pluripotent stem cells under highly defined condition. Sci Rep 2015;5:18550.

11 Shi Y, Kirwan P, Smith J et al. Human cerebral cortex development from pluripotent stem cells to functional excitatory synapses. Nat Neurosci 2012;15:477–486.

12 Espuny-Camacho I, Michelsen KA, Gall D et al. Pyramidal neurons derived from human pluripotent stem cells integrate efficiently into mouse brain circuits *in vivo*. Neuron 2013;77:440–456.

13 Thompson LH, Bjorklund A. Reconstruction of brain circuitry by neural transplants generated from pluripotent stem cells. Neurobiol Dis 2015;79:28–40.

14 Wernig M, Zhao JP, Pruszak J et al. Neurons derived from reprogrammed fibroblasts functionally integrate into the fetal brain and improve symptoms of rats with Parkinson's disease. Proc Natl Acad Sci USA 2008;105:5856–5861.

15 Rhee YH, Ko JY, Chang MY et al. Protein-based human iPS cells efficiently generate functional dopamine neurons and can treat a rat model of Parkinson disease. J Clin Invest 2011;121:2326–2335.

16 Hallett PJ, Deleidi M, Astradsson A et al. Successful function of autologous iPSC-derived dopamine neurons following transplantation in a non-human primate model of Parkinson's disease. Cell Stem Cell 2015;16:269–274.

17 Lukovic D, Moreno Manzano V, Stojkovic M et al. Concise review: Human pluripotent stem cells in the treatment of spinal cord injury. Stem Cells 2012;30:1787–1792.

18 Hao L, Zou Z, Tian H et al. Stem cell-based therapies for ischemic stroke. BioMed Res Int 2014;2014:468748.

19 Tang YH, Ma YY, Zhang ZJ et al. Opportunities and challenges: Stem cell-based therapy for the treatment of ischemic stroke. CNS Neurosci Ther 2015;21:337–347.

20 Denham M, Parish CL, Leaw B et al. Neurons derived from human embryonic stem cells extend long-distance axonal projections through growth along host white matter tracts after intra-cerebral transplantation. Front Cell Neurosci 2012;6:11.

21 Grealish S, Diguet E, Kirkeby A et al. Human ESC-derived dopamine neurons show similar preclinical efficacy and potency to fetal

neurons when grafted in a rat model of Parkinson's disease. Cell Stem Cell 2014;15:653–665.

22 Denham M, Bye C, Leung J et al. Glycogen synthase kinase 3beta and activin/nodal inhibition in human embryonic stem cells induces a pre-neuroepithelial state that is required for specification to a floor plate cell lineage. Stem Cells 2012;30:2400–2411.

23 Denham M, Dottori M. Neural differentiation of induced pluripotent stem cells. Methods Mol Biol 2011;793:99–110.

24 Thompson LH, Parish CL. Transplantation of fetal midbrain dopamine progenitors into a rodent model of Parkinson's disease. Neural Progenitor Cells: Methods and Protocols 2013;1059:169–180.

25 Thompson L, Barraud P, Andersson E et al. Identification of dopaminergic neurons of nigral and ventral tegmental area subtypes in grafts of fetal ventral mesencephalon based on cell morphology, protein expression, and efferent projections. J Neurosci 2005;25:6467–6477.

26 Cavalieri B. Geometric Degl: Indivisible. Editrice, Turin: Unione Tipografico, 1966.

27 Steinbeck JA, Koch P, Derouiche A et al. Human embryonic stem cell-derived neurons establish region-specific, long-range projections in the adult brain. Cell Mol Life Sci 2012; 69:461–470.

28 Steinbeck JA, Choi SJ, Mrejeru A, Ganat Y, Deisseroth K, Sulzer D, Mosharov EV, Studer L. Optogenetics enables functional analysis of human embryonic stem cell-derived grafts in a Parkinson's disease model. Nat Biotechnol 2015;33:204–209.

29 Eiraku M, Watanabe K, Matsuo-Takasaki M et al. Self-organized formation of polarized cortical tissues from ESCs and its active manipulation by extrinsic signals. Cell Stem Cell 2008;3:519–532.

30 Gaspard N, Bouschet T, Hourez R et al. An intrinsic mechanism of corticogenesis from embryonic stem cells. Nature 2008;455:351–357.

31 Koch P, Opitz T, Steinbeck JA et al. A rosette-type, self-renewing human ES cell-derived neural stem cell with potential for *in vitro* instruction and synaptic integration. Proc Natl Acad Sci USA 2009;106:3225–3230.

32 Avaliani N, Sorensen AT, Ledri M et al. Optogenetics reveal delayed afferent synaptogenesis on grafted human-induced pluripotent stem cell-derived neural progenitors. Stem Cells 2014;32:3088–3098.

33 Cunningham M, Cho JH, Leung A et al. hPSC-derived maturing GABAergic interneurons ameliorate seizures and abnormal behavior in epileptic mice. Cell Stem Cell 2014;15: 559–573.

34 Daadi MM, Maag AL, Steinberg GK. Adherent self-renewable human embryonic stem cell-derived neural stem cell line: Functional engraftment in experimental stroke model. PLoS One 2008;3:e1644.

35 Chen SJ, Chang CM, Tsai SK et al. Functional improvement of focal cerebral ischemia injury by subdural transplantation of induced pluripotent stem cells with fibrin glue. Stem Cells Dev 2010;19:1757–1767.

36 Nori S, Okada Y, Yasuda A et al. Grafted human-induced pluripotent stem-cell-derived neurospheres promote motor functional recovery after spinal cord injury in mice. Proc Natl Acad Sci USA 2011;108: 16825–16830.

37 Fujimoto Y, Abematsu M, Falk A et al. Treatment of a mouse model of spinal cord injury by transplantation of human induced pluripotent stem cell-derived long-term self-renewing neuroepithelial-like stem cells. Stem Cells 2012;30:1163–1173.

38 Gomi M, Takagi Y, Morizane A et al. Functional recovery of the murine brain ischemia model using human induced pluripotent stem cell-derived telencephalic progenitors. Brain Res 2012;1459:52–60.

39 Oki K, Tatarishvili J, Wood J et al. Human-induced pluripotent stem cells form functional neurons and improve recovery after grafting in stroke-damaged brain. Stem Cells 2012;30:1120–1133.

40 Mohamad O, Drury-Stewart D, Song M et al. Vector-free and transgene-free human iPS cells differentiate into functional neurons and enhance functional recovery after ischemic stroke in mice. PLoS One 2013;8:e64160.

41 Tornero D, Wattananit S, Gronning Madsen M et al. Human induced pluripotent stem cell-derived cortical neurons integrate in stroke-injured cortex and improve functional recovery. Brain 2013;136:3561–3577.

Author/s:
Niclis, JC; Turner, C; Durnall, J; McDougal, S; Kauhausen, JA; Leaw, B; Dottori, M; Parish, CL; Thompson, LH

Title:
Long-Distance Axonal Growth and Protracted Functional Maturation of Neurons Derived from Human Induced Pluripotent Stem Cells After Intracerebral Transplantation

Date:
2017-06-01

Citation:
Niclis, J. C., Turner, C., Durnall, J., McDougal, S., Kauhausen, J. A., Leaw, B., Dottori, M., Parish, C. L. & Thompson, L. H. (2017). Long-Distance Axonal Growth and Protracted Functional Maturation of Neurons Derived from Human Induced Pluripotent Stem Cells After Intracerebral Transplantation. STEM CELLS TRANSLATIONAL MEDICINE, 6 (6), pp.1547-1556. https://doi.org/10.1002/sctm.16-0198.

Persistent Link:
http://hdl.handle.net/11343/257579

File Description:
published version